SUPERNOVAE NEAR EARTH

ANA ŠUBIC

Fakulteta za matematiko in fiziko Univerza v Ljubljani

Some radioactive isotopes produced in massive stars and during supernovae have a sufficiently long decay time to provide information about events happening in our surroundings even millions of years ago. The spectral line of aluminum-26 is bright enough to allow its abundance in the Galaxy to be measured across different regions, while iron-60 is the most suitable choice when searching for the ejected material deposited on Earth. Such supernovae must have occurred within approximately 100 parsecs, making it possible that they had an impact on Earth. This article summarizes the results of various studies suggesting that at least three supernova explosions took place in our recent past: approximately 1.8 million years ago, around 2.5 million years ago, and 6.5–8.7 million years ago.

ZEMLJI BLIŽNJE SUPERNOVE

Nekateri radioaktivni izotopi, ki nastajajo v masivnih zvezdah ter med eksplozijami supernov, imajo dovolj dolg razpadni čas, da nam o dogodkih v naši okolici pričajo še milijone let kasneje. Spektralna črta aluminija-26 je dovolj izrazita, da se njegovo zastopanost v Galaksiji lahko meri tudi v različnih območjih, železo pa je najprimernejša izbira, ko iščemo izvrženi material supernov odložen na Zemlji. Takšne supernove so se morale zgoditi na razdalji do približno 100 pc, zato je možno, da so imele vpliv na Zemljo. Članek povzema rezultate številnih raziskav, ki nakazujejo, da so se v naši bližnji preteklosti zgodile vsaj tri eksplozije supernov: pred približno 1.8 milijoni let, pred približno 2.5 milijoni let in pred 6.5–8.7 milijoni let.

1. Introduction

Supernova explosions occur in our Galaxy between once and three times per century (1.54 ± 0.89) [1]. Much more rarely, they happen in Earth's local vicinity (e.g., within approximately 100 pc or roughly 325 light-years), therefore such events have sparked curiosity for decades: have they ever occurred in the past, and if so, how did they affect Earth?

A strong piece of evidence for nearby supernovae comes from radioisotopes that traveled to our Solar System in the millennia following the explosions of supernovae. They were deposited homogeneously — both on Earth, for example in layers of oceanic sediments or polar ice, as well as on the Moon. Particularly useful is the heavy iron isotope ⁶⁰Fe with a half-life of 2.6 million years, which has been proven to reach Earth in non-negligible amounts exclusively from supernovae. The age of the sediment in which iron-60 decay events were detected is determined using another well-known radioisotope, such as beryllium.

When identifying supernovae that occurred more than ten million years ago, decay events are no longer relevant, as the radioactive isotopes have largely decayed into stable ones. Searching for older explosions requires considering multiple assumptions — both about the frequency of nearby supernovae as our Solar System moves through galactic regions with different densities, and also about the impact of supernovae on Earth's climate. Assuming that supernovae ejecta have primarily cooling effect on Earth's atmosphere and that the frequency of supernovae is higher in denser regions of the Galaxy, a recent study reconstructed past explosions by studying Earth's short-term cooling events, in case they coincided with the Solar System's passage through denser regions of the Galaxy. It is however difficult to rule out that short-term cooling episodes were not (at least partially) triggered by other factors, such as volcanic eruptions or meteorite impacts.

The goal of this paper is to present the discovery of several supernovae in past, along with the associated questions that still persist. I will introduce the relevant types of supernovae with

© (2025 The Author(s). Original content from this work may be used under the terms of the Creative Commons Attribution 4.0 licence.

the nuclear reactions that make them recognizable, and also describe some recent changes in the local environment of our Solar System. The methods examined in this paper also includes multiple measurements of the half-life of iron-60 and the effective detection of extremely small samples of this isotope using mass spectrometry. Finally, I will discuss theories on how nearby supernovae have influenced Earth's biodiversity.

2. Properties of relevant radioisotopes

Detection and dating of supernovae near Earth through radioisotopes is a robust method, as it does not rely on not yet fully proven hypotheses or potentially oversimplified simulations, and neither on indirect astronomical observations. The main goal of such research is to identify an isotope that is produced predominantly in supernovae rather than through other cosmic-ray interactions with matter. If we are searching for it on Earth, the isotope must have a short enough half-life, so that its primordials – samples that were present on the Earth since its formation – do not interfere with the measurements. At the same time, half-life must be long enough for isotopes to survive the journey from the supernova to Earth without fully decaying into stable isotopes [2]. Supernovae are most commonly studied using the isotopes 26 Al, 53 Mn, and 60 Fe, which have suitable half-lives, denoted $\tau_{1/2}$, of 0.71, 2.62, and 3.7 million years. Radioactive isotopes produced by supernovae are also useful beyond just those decaying on Earth: their characteristic emission lines allow us to study their abundance in space, providing insights into the frequency of more distant supernovae.

2.1 Bright aluminum-26

Aluminum-26 ($\tau_{1/2} = 0.71 \cdot 10^6$ years) is produced in the cores of stars heavier than 8 times the mass of the Sun (M_{\odot}). The majority of it is created by massive stars (M > $10M_{\odot}$), which, after their core collapse phase, explode as type II supernovae (core-collapse supernovae, CCSNe). Another type of Al-26 producers are super-AGB stars: these are stars with masses $\sim 5M_{\odot} < M < 9M_{\odot}$, which are similar to red giants in their characteristics¹. According to the Super-AGB hypothesis, which explores possible origins of many short-lived isotopes in early Solar System and aligns with the radioactivity of certain meteorites, 3-10% of ²⁶Al is also produced in super-AGB stars that do not necessarily end their life as supernovae [4, 5].

Bellow is the formula showing decay process of aluminum-26. Its signature photon at 1.809 MeV is only emitted when its descendant magnesium-26' isomer (a state of an atom where only a nucleus is excited, which can last years) transitions into its ground state:

$$^{26}_{13} \text{Al} \quad \xrightarrow{\tau_{1/2} = 7,17 \cdot 10^5 \text{ years}} \quad ^{26}_{12} \text{Mg}^* + e^+ + \nu \quad \rightarrow \quad ^{26}_{12} \text{Mg} + \gamma. \tag{1}$$

The spectral line at 1.809 MeV can be measured accurately: long decay time assures us that enough time has passed since the supernova explosion for its material to spread out in space, making it transparent to gamma rays. If supernova material still remained dense at the time of radioisotopes' decay, gamma rays could be absorbed by it and then emitted at different wavelengths, supernovae-specific spectral lines thus being destroyed. The long decay time also means that the material no longer travels at too high of a speed (after 10⁵ years, only a few tens of km/s) — thus, Doppler broadening of the spectral lines can be treated in a non-relativistic approximation [6]. The expression connects the spectral distribution over wavelengths with the probability distribution of

¹ESA/Hubble Word Bank explains that "a red giant forms after a star has run out of hydrogen fuel for nuclear fusion in its core, and has begun the process of dying" [3]. This happens to stars with a mass between $0.8M_{\odot}$ and $8M_{\odot}$. Such star then burns hydrogen in its shell, which makes it expand and cool down afterwards, forming a bigger star with a relatively red light spectrum. Such stars are not massive enough to explode as a supernova, but end their life as a planetary nebulae instead.

the material's velocity in the direction of the observer, P_v , where we have expressed the velocity towards the observer in terms of the wavelength shift $c(1 - \lambda/\lambda_0)$, λ_0 denoting wavelength at the point of origin and c denoting speed of light:

$$P_{\lambda}(\lambda) d\lambda = \frac{c}{\lambda_0} P_v \left[c \left(1 - \frac{\lambda}{\lambda_0} \right) \right] d\lambda. \tag{2}$$

At energies in the megaelectronvolt range, the lines are therefore broadened by less than 3 keV at FWHM (full width at half-maximum) [7]. Full width at half-maximum of predominately Gaussian distribution is related to the standard deviation and is often used in spectrometry and laser physics as it describes the width of a spectral line [8]. Long decay times are important since they allow the ejected isotopes' speed to decrease first, thus keeping emission lines narrow and recognizable when observing from Earth. On the other hand, long decay time means ejected aluminum-26 had time to spread, so the origin of its emission line is not point-like but diffusely illuminates the interstellar space [7]. Since well-established models assume that approximately $10^{-4} M_{\odot}^{26}$ Al is released in each outburst [2], we can still calculate from the number of decays how many supernova explosions have occurred in the isotopically relevant past (the last million years). Additional confidence in the 26 Mg/ 26 Al ratio derived from spectral line at 1.809 Me comes from the fact that aluminum will almost certainly decay into isomeric 26 Mg*, as the decay directly to the ground state of magnesium only occurs from the nuclear isomer of aluminum [7]. Since it is highly unlikely for an aluminum nucleus to be in an excited state in interstellar space on its own, we can safely conclude that the amount of 26 Mg transitions to the ground state corresponds to the previous amount of 26 Al.

The aluminum line is so bright that it can even be measured regionally within our Galaxy using satellites [1]. The emission at 1.809 MeV occurs with 100% probability (and with 4% at 1.130 MeV) [7]. However, there is some uncertainty surrounding the reliability of this radioisotope's formation, especially when compared to the isotope iron-60 [9].

2.2 Less bright and more rare iron-60

Iron-60 ($\tau_{1/2} = 2.62 \cdot 10^6$ years) is primarily produced in extremely massive stars, partially during the supernova explosion, but mainly in the shell burning phase when the massive star runs out of hydrogen in its core and starts burning the one in its shell, later transitioning to burning heavier and heavier product elements as fuel. This is soon followed by core collapse and a type II supernova [1]. Such iron-60 origin is safe to assume because the half-life of its precursor, ⁵⁹Fe, is only 44.5 days, meaning that a high neutron density is required for double neutron capture within a relatively short timescale [10]. Like aluminum-26, a smaller fraction (3-10%) of iron-60 can also be produced in super-AGB stars [4, 5].

Iron-60 decays into cobalt-60 ($\tau_{1/2} = 5.27$ years), which then rapidly undergoes β^- decay into nickel-60. When the excited nickel transitions to its ground state, two photons are emitted in a cascade with characteristic energies of 1.173 and 1.3325 MeV:

2.3 Comparision of both isotopes

The two iron spectral lines from the cascade decay of cobalt in the Galaxy reach only 15% of the intensity of the aluminum line [1] and cannot be localized, which is why aluminum remained the focus of historical observations for a long time (iron-60 only started receiving more attention in

the 1980s). On the other hand, iron-60 is much more useful when searching for traces of nearby supernovae directly on Earth, as aluminum-26 is also produced in the atmosphere through cosmic-ray collisions with argon, at a rate of $(1.1 \pm 0.3) \cdot 10^{-4}$ atoms $cm^{-2}s^{-1}$ [2, 11].

For the most reliable results, the decays of both radioisotopes are often detected and compared to see whether the measured ratio matches predictions — both on Earth and in the Galaxy. In 2002, two satelites were launched that provided us with crucial data for further research: those were ESA's mission Integral and Nasa's RHESS, depicted on Figures 1 and 2. Integral (the name comes from INTErnational Gamma-Ray Astrophysics Laboratory) was the first space observatory to simultaneously observe objects in gamma rays, X-rays, and visible light. Its principal targets were gamma-ray outbursts as supernova explosions as well as regions with black holes [12]. Its mission was completed during the writing of this article in February 2025. The RHESSI mission (Reuven Ramaty High Energy Solar Spectroscopic Imager) by NASA mainly focused on solar events, which was done by observing gamma ray emissions and high energy events, among other methods [13].

The observations of aforementioned satelites have provoked further questions: theoretical models suggest that the $^{60}\text{Fe}/^{26}\text{Al}$ ratio in our Galaxy should be up to twice as high as what has been measured, although the measured intensity is still within the uncertainty range [1]. This is also relevant for nearby supernovae, as a significantly skewed ratio could indicate that aluminum-26 is produced in non-negligible amounts independently of supernovae — meaning there may be fewer of the explosions, or that they evolve differently than expected.



Figure 1. ESA's satellite Integral that simultaneously observed objects in gamma rays, X-rays and visible light.

Image taken from ESA, [12].



Figure 2. NASA's satellite RHESSI that mainly focused on observing gamma ray emissions and high energy events. Image taken from [13].

The reasons for this discrepancy vary, and there are likely multiple contributing factors. One possible explanation is that aluminum-26 is produced in several different late-stage shell burning phases, and is expelled into the surrounding medium through stellar winds, whereas iron-60 is released exclusively through supernova explosions. In this case, the supernova rate itself would not be overestimated, but aluminum would have more time to spread through space. Another possible reason involves Wolf-Rayet stars. These really massive stars (> $40M_{\odot}$) with specific and unusual spectra are defined by their depletion of hydrogen and extreme solar winds [2]. They lose part or even all of their outer envelope due to strong radiative pressure before reaching the end of their life cycle [2]. Wolf-Rayet stars produce aluminum-26 but not iron-60 [9], even though they also explode as supernovae at the end, which makes them a potential major source of aluminum-26. On the other hand, iron-60 is also produced in electron-capture supernovae (ECSNe), which according to models should not be a significant source of aluminum-26 [5]. These are stars with masses in the range $8M_{\odot} < M < 10M_{\odot}$, but so far, only a few supernovae have been identified as candidates for

ECSN [14], meaning there may be too few of them to contribute significantly to iron-60 production. Reynold Diehl, in his article [1] discussing findings from ESA's INTEGRAL satellite, suggests additional possible reasons for the discrepancy: models of massive stars may have overestimated neutron capture rates, leading to an overproduction of 60 Fe relative to the other iron isotopes. Stellar convection might need to be modeled differently. The number of truly massive stars in our vicinity may be too low for a statistically representative distribution. While most of the Earth's nearest supergiants take part in smaller and open OB associations (associations of tens to ~100 young bright stars that are not strongly gravitationally bound), supergiants in general can often be found in clusters, which makes the distant ones difficult to observe [1]. Another possibility is that some models used $\tau_{1/2}=1.49$ million years, measured in 1984 [15], which was invalidated by later experiments. In any case, both the galactic and terrestrial 60 Fe/ 26 Al ratio appears to be consistently around 0.15–0.18 [1, 5], meaning that stellar evolution and interstellar dust models will need to adapt accordingly.²

3. Determining the half-life of iron-60

The probability of reactions that require capturing particles (e.g. neutrons, electrons) depends on the density of those particles, but that is not the case for the decay of iron-60. In contrast to decays that also occur via electron capture, β^- decay of iron-60 provides us with a "clock" independent of its surroundings – actions will happen regardless of the density of matter around the isotope which makes it an appropriate reaction for reconstructing supernova emissions. For such use, its half-time is of crucial importance [10]. For an element that only exists in trace amounts on Earth, getting to the precise value proved to be challenging. While reviewing the literature, we come across different values for the half-life of iron-60: for example, the often-cited papers on the discovery of iron-60 in deep-sea sediments from 2004 [16] and 2008 [17] still used $\tau_{1/2} = 1.49$ million years, a value published in 1984 [15]. The updated half-life value of $\tau_{1/2} = 2.62$ million years was published in 2006 by G. Rugel and colleagues, and was later confirmed by A. Wallner's group in 2015 with a refined value of $\tau_{1/2} = 2.50$ million years [10].

Let's consider the last method, described in [10], for determining $\tau_{1/2}(^{60}\text{Fe})$. If we know the decay activity of the isotope A_{60Fe} and simultaneously the number of atoms of iron-60 in the sample, N_{60Fe} , we can determine the half-life as:

$$\tau_{1/2}(^{60}\text{Fe}) = \ln 2 \cdot N_{60Fe} / A_{60Fe}.$$
 (4)

In the case of iron-60, the activity is measured through the aforementioned spectral lines at 1.173 MeV and 1.332 MeV, which correspond to the decay of the daughter isotope 60 Co. The relationship between the intensities of the two signature rays A(t) at 1173 keV and 1332 keV is described by the approximation [10], where A_0 is the activity of cobalt-60 at t=0, $A_{60\text{Fe}}$ denotes iron-60 activity, and λ is a cobalt-60 decay constant:

$$A_{1173} = 0.9985[A_0e^{-\lambda t} + 0.9975A_{60\text{Fe}}(1 - e^{-\lambda t})], \tag{5}$$

$$A_{1332} = 0.9998[A_0e^{-\lambda t} + A_{60\text{Fe}}(1 - 0.9975e^{-\lambda t})]. \tag{6}$$

The activity of radioisotopes can be measured precisely, which led to the conclusion that the significant difference between the previous two measurements stemmed from the determination of

²Interstellar dust (usually in size of μm) acts as a radioisotope carrier as single atoms would not survive all the way from supernova to Earth. Since different size and material of dust affect isotopes' travel times and its sensitivity to the magnetic fields, dust models play as important role as stellar evolution models do in reconstructing the origins of supernovae ejecta [2].

the number of iron-60 atoms in the sample. As with the first half-life measurement, Wallner's research group [10] approached this by using accelerator mass spectrometry (AMS), the most common method for measuring isotopes in trace amounts: the sensitivity of the best spectrometers reaches ratios as low as 10^{-18} of the target isotope relative to the remaining material. While approximately two-thirds of the iron-60 sample was used for a four-year activity measurement, the remainder was analyzed using two different spectrometers. Those were Vienna Environmental Research Accelerator – VERA at Vienna and Accelerator mass spectrometer at Australian National University – AMS ANU. The ingenuity of the last spectrometer usage was the calculation of the iron-60 content using the number density relative to the radioisotope 55 Fe ($au_{1/2}=2.744$ years). In contrast to previous measurements that focused on the ⁶⁰Fe/^{nat}Fe ratio, where ^{nat}Fe denotes naturally occurring iron (essentially ⁵⁴Fe, ⁵⁶Fe, ⁵⁷Fe, ⁵⁸Fe in their natural abundances), Wallner's group was now working with an isotope of similarly low abundance as a reference point. In this approach, the ⁵⁵Fe/^{nat}Fe ratio was measured on both spectrometers, while the ⁶⁰Fe/^{nat}Fe ratio was measured only at the Australian National University's heavy-ion accelerator, which is the only device capable of distinguishing iron-60 from the nickel-60 background. Since the AMS results were standardized using stable ⁵⁶Fe standards, and these standards are also based on the half-lives of iron isotopes, it was logical to use the ratio of two low-abundance radioactive isotopes to minimize systematic uncertainties as much as possible.

In the end, the number of 60 Fe atoms N_{60} was determined as the average of the results from two independent equations that deal with four different samples containing both iron-60 and iron-55. Fe-1 was the sample used in its original from, while in samples Fe-2, Fe-3 and Fe-4, radioisotopes 55 Fe and 60 Fe were diluted with a stable and most common isotope 56 Fe by factor 10, 100 and 1000 to increase predictability of the measurements. In Equation 7, different measurement techniques of atom numbers in the four samples, and then combining their ratios to retrieve the N_{60} are meant to minimize mistakes at mass spectrometry, while in the Equation 8, the number of 60 Fe is based on the activity of more short-lived 55 Fe:

$$N_{60}(\text{Fe-1}) = \frac{R_{60/56}(\text{Fe-4})}{R_{55/56}(\text{Fe-4})} \cdot \frac{R_{55/56}(\text{Fe-4})}{R_{55/56}(A_{55})} \cdot R_{55/56}(A_{55}) \cdot N_{56}(\text{Fe-4}) \cdot \frac{N_{55}(\text{Fe-1})}{N_{55}(\text{Fe-4})}, \tag{7}$$

$$N_{60}(\text{Fe-1}) = A_{55}(\text{Fe-1}) \cdot \frac{\tau_{1/2}(^{55}Fe)}{\ln 2} \cdot \frac{N_{60}}{N_{55}}.$$
 (8)

Equation 7 combines the ratios of isotopes obtained in different ways, where $R_{x/y}$ denotes the numerical density of the isotope in the Fe-1 or Fe-4 sample obtained via AMS, and A_{55} indicates that the ratio was derived from the measurement of 55 Fe activity and calculated using standard contents of 55 Fe/ 56 Fe. Equation 8 expresses the number of 60 Fe directly from the radioactive decays of iron-55 in the Fe-1 sample, where N_{60}/N_{55} is the ratio of the ratios $R_{60/56}$ (Fe-4)/ $R_{55/56}$ (Fe-4). The activity of iron-55 was measured using liquid scintillation counting (LSC).

The average value of both results [10], which represents the final number of iron-60 atoms, was $2.47 \cdot 10^{15}$ atoms (equivalent to just 0.245 µg!). Based on the four-year activity measurement $A_{60Fe} = 21.72 \text{ s}^{-1}$ and using Equation 10, the latest half-life of iron-60 is $(2.50 \pm 0.12) \cdot 10^6$ years. The authors propose using a weighted average of their result and the previous one, leading to $\tau_{1/2} = (2.60 \pm 0.05) \cdot 10^6$ years.

³In LSC, the energy of each decay is transferred into photons emitted by scintillators, which are then transferred into electric signals using photomultiplier tubes. This enables reliable measurements of radioactive activity, since the counting of electrical pulses can be carried out with high precision.

Supernovae near Earth



Figure 3. A nodule is a geological term for rock formations of a round shape that form on the ocean floor when minerals, primarily manganese oxides, slowly adhere to the solid rocks in the core. If they contain ferromanganese (FeMn) nodules. Picture taken from [21].

4. Discovery of nearby supernovae through isotopes on Earth

Detections and examinations of radioisotopes as traces of the supernovae in the local vicinity of our Solar System have already been tackled by several research groups. An established method involves studying several meters thick sediment layers, dating the age of the layers using beryllium-10, and finally determining the ⁶⁰Fe/Fe ratio through accelerator mass spectrometry, with counting decay events being useful for confirming the measured abundance. Each new research project has introduced some new approach or sample. In Table 1, we can observe a comparison of iron-60 abundance with other radioactive, non-primordial isotopes or unusual sample types. There have been a study of nodules [18] from the Atlantic Ocean (Figure 3), detections of the isotope in lunar samples [19], and detection of iron-60 deposition in relatively fresh Antarctic snow — in this way, the group [20] demonstrated that interstellar iron-60 is still being deposited on Earth at present.

The results of seven such studies [16, 17, 18, 22, 19, 5, 20] are collected in Table 1:

Table 1. A review of studies on iron-60 in various samples. The ages of layers with increased radioisotope abundance are in good agreement with each other.

Publication	Isotopes	Location and form of the sample	Fe Layer Age
K. Knie, 2004	⁶⁰ Fe	Feromanganese crust (Equatorial Pacific)	2.4 - 3.2 mil. yr
C. Fitoussi, 2008	60 Fe	same sample as in Knie, 2004	without findings
A. Wallner, 2016	60 Fe	FeMn crust (Equatorial Pacific), FeMn nodules	1.5 - 3.2 and
		(Southern Atlantic), sediments (Indian ocean)	6.5 - 8.7 mil. yr
P. Ludwig, 2016	60 Fe	Sediment (Equatorial Pacific)	1.7 - 2.8 mil. yr
L. Fimiani, 2016	60 Fe, 53 Mn	lunar samples, Missions Apollo 12, 15, 16	1.7 - 2.6 mil. yr
J. Feige, 2016	60 Fe, 26 Al	Sediments (Indian Ocean)	1.7 - 3.2 mil. yr
D. Koll, 2016	60 Fe, 53 Mn	Snow layers (Antarctica)	0 - 20 yr

The most extensive study from 2016 [18], which included samples from all three oceans, not only identified a more recent event but also discovered an increased deposition of iron-60 on Earth from 6.5 to 8.7 million years ago, indicating (at least) two supernova explosions at a distance of ~ 100 pc within the past 10 million years. Their results about isotope ratios as a function of temporal distance are shown in Figure 4. The elevated concentrations for the older supernova indicate (0.38 ± 0.09) instead of $(0.15 \pm 0.11) \cdot 10^{-15}$ ⁶⁰Fe/^{nat}Fe which was their base level, demonstrating the exceptional precision of AMS. A look at the age of layers with increased iron-60 abundance shows that both this one and other studies to date are in good agreement. An exception is the 2008 study, which failed to reproduce the detection of iron-60 in a sample from 2004. With three significant findings of increased radioisotope abundances – one dating back 6.5 to 8.7 million years, another between

1.7 and 3.2 million years ago, and an above-average influx in the present – it naturally raises the question: can we identify the corresponding supernovae?

According to models, iron-60, which reaches Earth in the form of micron-sized dust grains, would travel much slower than light from a supernova located around 100 pc away (1 pc = 3.26 light-years), taking between 200,000 and roughly a million years to arrive [18, 2]. Smaller particles, such as individual atoms, cannot penetrate Earth's atmosphere [2]. The relatively long traveling time means that, in order to reconstruct the origin of the supernova, we must also consider the movement of the Solar System, that is orbiting the Galactic center at approximately 230 km/s.

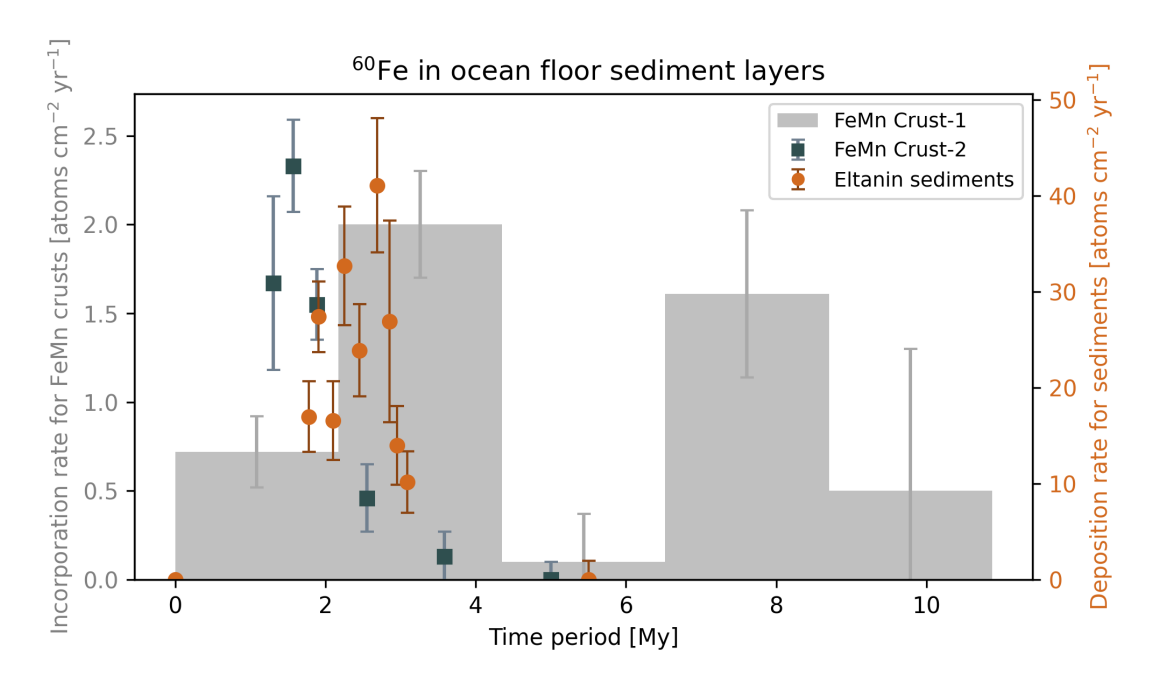


Figure 4. Results from the most extensive detection of ⁶⁰Fe to date, combining samples from three oceans. Both the incorporation rates and concentrations for each sample are displayed. Figure prepared by Ana Šubic using publicly available research data [18].

The Sun is currently part of our Local Bubble, a region approximately 100 pc in size with lowerdensity but ionized (hotter) gas. The ionization suggests hot events in the not so distant past — it is estimated that The Local Bubble was created by multiple supernovae within the last 14 million years [18]. Recent model results from 2023 [23] indicate that, about 6.5 million years ago, the Sun was still part of another bubble, likely the Orion-Eridanus Superbubble, in the nearby constellations of Taurus, Orion, and Centaurus, and that the first explosion occurred in this region [2]. Another explosion likely occurred around 2.5 million years ago, probably in the direction of Serpens [2], with the Sun entering the Local Bubble about 4.6 million years ago [23]. Within this region, the Sun is currently moving through the denser Local Interstellar Cloud (LIC), which it is expected to exit in the next few thousand years. Afterwards, the Sun will likely enter the G-Cloud, which is also moving toward the Solar System. Both of these denser clouds are approximately 2-4 pc in size. In the recent study of freshly accumulated iron-60 from Antarctica, Feige and colleagues [5] explain that the latest influx of iron-60 significantly increased when the Sun entered the Local Interstellar Cloud and shoved into material. There is also the finding that about 1.8 million years ago, the pulsar PSR B1706-16 and the star Zeta Serpentis were sent off in opposite directions. Their violent escape from a common origin suggests that they were once a binary star system. A gravitationally bound system like this could only have been disrupted by something as powerful as a nearby supernova. Considering that radioactive isotopes had to travel to the Solar System for approximately a million years, this could explain the recent increase in the deposition of iron-60, which continues on Earth

today [2].

5. A possible impact of supernovae on life on Earth

Professor Zwitter reminds us in his book [2] that the early human species, which existed as early as 1.8 million years ago, apparently survived the last nearby supernova event. That was the time of Homo habilis. Towards the end of this paper, I would like to offer the perspective of H. Svensmark, who in his work [24] explains how nearby supernovae might even benefit Earth's biodiversity. Given that life on Earth has existed for about 3.7 billion years, analyzing only the data about recent supernovae is insufficient; through modeling the movement of the Solar System through the Galaxy, Svensmark examined the last 500 million years. The main assumption in determining our space environment was that the density of supernovae is higher within the main arms of the Galaxy, and as the Solar System travels between them, there will be fewer in its local vicinity. However, one more assumption was necessary: would the presence of a nearby supernova heat or cool the Earth? He assumed that the impact of supernovae would mostly be cooling, as they introduce more condensation nuclei into the atmosphere, and for the following several millennia, Earth would have increased cloud coverage at mid-altitudes. Cloud coverage at such altitudes would increase albedo of Earth's atmosphere more than it would cause a green-house effect, resulting in a cooling effect [24].

Now to biodiversity: biologists suggest it tends to increase during cooler climatic periods. In warmer conditions, dominant species prevail, limiting the spread of others, while during cooler periods, the dominant species weakens, letting less prominent species to evolve more freely. In cooler climates, the temperature gradient between the Tropics and the Polar Circle is greater, which creates wider range of habitats and consequently more diverse ecosystems. On the other hand, great importance has been attributed to the amount of water bodies and coastal regions: more fragmented and wetter continents offer more heterogeneous living environments. Since the amounts of liquid waters and coastline fragmentations are dependent both on tectonics and climate, even warmer climates benefit as they raise sea levels and flooding becomes more common [24]. The combination of graphs in Figure 5 shows the biodiversity of genera in relation to the historic sea level. It is clear that sea level alone cannot fully explain the biodiversity trends. Svensmark therefore considered parameters: sea level height relative to present-day levels and the modeled supernova density in the surrounding region within 500 pc.

According to his hypothesis, one could fit the ever changing number of genera N(t) to the historic sea level values Λ (sea level, t) and to the function of supernovae density rate $\Gamma(SN, t)$ as

$$N(t) = \Gamma(SN, t)\Lambda(\text{sea level}, t) + \epsilon(t), \tag{9}$$

where $\epsilon(t)$ is a noise term. Since both the number of genera and historic sea level can be relatively well reconstructed through fossil examinations and other methods, they can be combined to a genera count, normalized to the sea level as $N(t)/\Lambda$ (sea level, t). The latter should then match with the supernovae density, as it is modeled according to the Solar System passing through more and less dense space of the Galaxy – with more explosions to happen in the midst of Galaxy's main arms, and with the model taking into the account that diffusion only provides the Earth's atmosphere with clear spike of cosmic rays if the supernova explosion occurs sufficiently close both in time and space – a full review of the model's parameters is beyond the scope of this article and can be found in [24]. The farther we move in time from dense supernovae regions, the less beneficial should the climate become and the lesser the number of genera; however, since the rebuild of the biodiversity after the mass extinction takes from 10 to 40 million years, there is a temporal shift included in the model,

where the effects of the supernova follow with a delay of $\lambda(t-t')$. At the end, all the measured terrestrial quantities are set on the left side of the equation whereas all the celestial quantities being used to model the supernovae rate are on the right side of the equation with two constants ν_1 and ν_2 . The equation to predict the changes of biodiversity is then

$$\frac{N(t)}{\Lambda(\text{sea level}, t)} = \nu_1 \int_{-\infty}^{t} SN(t') \exp[-\lambda(t - t')] dt' + \nu_2 + \epsilon(t). \tag{10}$$

The result is shown in Figure 6, where the left side of the equation is blue colored, and the model of the right side of the equation is a thin black line. The gray area represents the 1σ variance of the model.

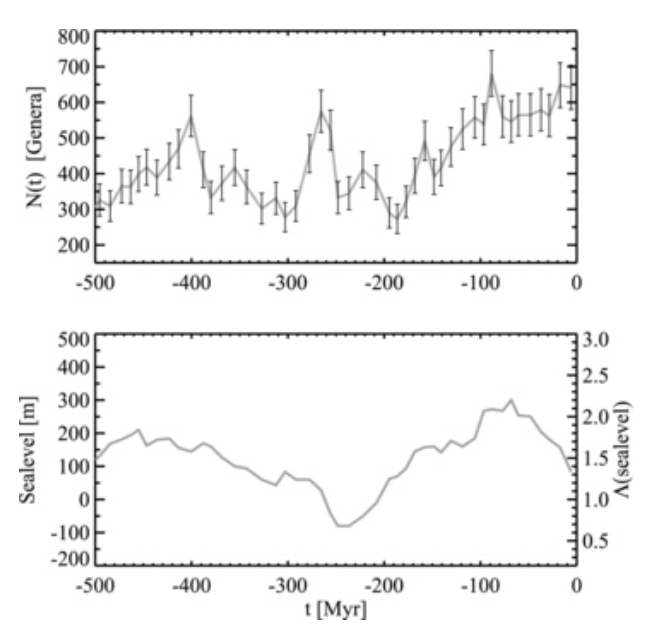


Figure 5. Comparison of biodiversity (number of genera) and sea level height, taken from [24].

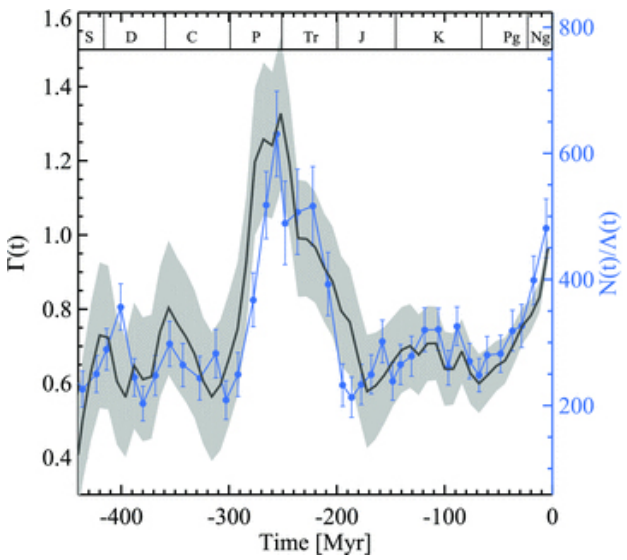


Figure 6. The black line: predicted movement of biodiversity (number of genera), normalized to sea level height, calculated based on the supernova density. The blue line represents the generally accepted change of the number of genera, again normalized to sea level height.

Taken from [24].

6. Conclusion

Radioactive activity in space continues to be an important topic of research, and the ratios between isotopes provide useful boundary conditions for modelling supernovae and the general development of the Galaxy. This paper focuses on the detection of the radioisotopes iron-60 and aluminum-26 on Earth and in space through spectral lines. For accurate calculations of isotope abundance based on decay events, it is essential to have precise knowledge of their half-lives. In the case of iron-60, the results have not always been consistent, so we discussed the most recent measurement using accelerator mass spectrometry. Finally, we examined the timing and origin of the last three supernovae. The effects of supernovae on Earth's climate and biodiversity are another topic worth exploring, but we must remain as conservative as possible with our assumptions. It would be interesting to see how well models of past supernovae align with other biodiversity indicators, not just with the number of genera, and to use more complex reconstructions of the Galaxy. It would also be sensible to consider different types of radiation, shock waves, and particles, both immediate and delayed effects, since each explosion involves a combination of everything from dust particles to gamma radiation.

Supernovae near Earth

REFERENCES

- [1] R. Diehl, Nuclear astrophysics lessons from INTEGRAL, Rep. Prog. Phys. 76 (2013), 026301.
- [2] T. Zwitter, Zvezde, osončja in njihovo opazovanje, Univerza v Ljubljani, Fakulteta za matematiko in fiziko, Verzija 1. september 2024, 2024.
- [3] T. E. S. Agency, Word bank: red giant, July 2012, https://esahubble.org/wordbank/red-giant/, accessed on 16.8.2025.
- [4] M. Lugaro et al., Short-lived radioactivity in the early Solar System: the Super-AGB star hypothesis, Meteorit. Planet. Sci. 47 (2012), 1998–2012.
- [5] J. Feige et al., Limits on supernova-associated ⁶⁰Fe/²⁶Al nucleosynthesis ratios from accelerator mass spectrometry measurements of deep-sea sediments, Phys. Rev. Lett. **121** (2018), 221103.
- [6] Doppler broadening, Wikipedia, https://en.wikipedia.org/wiki/Doppler_broadening, accessed on 24.2.2025.
- [7] R. Ramaty and R. E. Lingenfelter, ²⁶Al: a galactic source of gamma-ray line emission, The Astrophysical Journal 213 (1977).
- [8] Dan, Spectral line measurements visualized, Mar. 2012, https://bdnyc.org/blog/2012/03/02/spectral-line-measurements-visualized/, accessed on 1.5.2025.
- [9] N. Prantzos, Radioactive ²⁶Al and ⁶⁰Fe in the Milky Way: implications of the RHESSI detection of ⁶⁰Fe, Astron. Astrophys. 420 (2004), 1033–1037.
- [10] A. Wallner et al., Settling the half-life of ⁶⁰Fe: fundamental for a versatile astrophysical chronometer, Phys. Rev. Lett. 114 (2015), 041101.
- [11] J.-L. Reyss et al., Production cross sections of ²⁶Al, ²²Na, ⁷Be from argon and of ¹⁰Be, ⁷Be from nitrogen: implications for production rates of ²⁶Al and ¹⁰Be in the atmosphere, Earth Planet. Sci. Lett. **53** (1981), 203–210.
- [12] T. E. S. Agency, Mission accomplished for Integral, ESA's gamma-ray telescope, Feb. 2025, https://www.esa.int/Science_Exploration/Space_Science/Integral/Mission_accomplished_for_Integral_ESA_s_gamma-ray_telescope, accessed on 1.5.2025.
- [13] N. Aeronautics and G. S. F. C. Space Administration, *RHESSI mission archive*, Apr. 2018, https://hesperia.gsfc.nasa.gov/rhessi3/mission-archive/index.html, accessed on 1.5.2025.
- [14] D. Hiramatsu, The electron-capture origin of supernova 2018zd, Nat. Astron. 5 (2021), 903-910.
- [15] W. Kutschera et al., Half-life of ⁶⁰Fe, Nucl. Instrum. Methods Phys. Res. B 5 (1984), 430–435.
- [16] K. Knie et al., ⁶⁰Fe anomaly in a deep-sea manganese crust and implications for a nearby supernova source, Phys. Rev. Lett. 93 (2004), 171103.
- [17] C. Fitoussi et al., Search for supernova-produced ⁶⁰Fe in a marine sediment, Phys. Rev. Lett. 101 (2008), 121101.
- [18] A. Wallner et al., Recent near-Earth supernovae probed by global deposition of interstellar radioactive ⁶⁰Fe, Nature **532** (2016), 69–72.
- [19] L. Fimiani et al., Interstellar ⁶⁰Fe on the surface of the moon, Phys. Rev. Lett. **116** (2016).
- [20] D. Koll et al., Interstellar ⁶⁰Fe in Antarctica, Phys. Rev. Lett. **123** (2019), 072701.
- [21] K. Mizzel, What's in a nodule?, Aug. 2021, https://oceanexplorer.noaa.gov/okeanos/explorations/ex2104/features/nodule/welcome.html, accessed on 1.3.2025.
- [22] P. Ludwig et al., Time-resolved 2-million-year-old supernova activity discovered in Earth's microfossil record, Proc. Natl. Acad. Sci. U. S. A. 113 (2016), 9232–9237.
- [23] M. Schulreich et al., Numerical studies on the link between radioisotopic signatures on Earth and the formation of the Local Bubble, Astron. Astrophys. **680** (2023), A39.
- [24] H. Svensmark, Evidence of nearby supernovae affecting life on Earth, Mon. Not. R. Astron. Soc. 423 (2012), 1234–1253.